

The urban climate of the largest cities of the European Arctic

Victoria Miles^{a,*}, Igor Esau^{b,a}, Martin W. Miles^{c,d}

^a Nansen Environmental and Remote Sensing Center, Bjerknes Centre for Climate Research, Bergen, Norway

^b Institute of Physics and Technology, UiT, The Arctic University of Norway, Tromsø, Norway

^c NORCE Norwegian Research Centre, Bjerknes Centre for Climate Research, Bergen, Norway

^d Institute of Arctic and Alpine Research, University of Colorado, Boulder, USA.

ARTICLE INFO

Keywords:

Arctic
Fennoscandia
Boreal
Urban heat island
Population
NDVI
Land surface temperature
Microclimate
MODIS

ABSTRACT

Recent studies have found intense and persistent positive temperature anomalies associated with urban areas in high northern latitudes. However, understanding the intensity and variability of urban heat islands (UHI) in these regions remains limited. Here we study the urban climate of the seven largest cities in the European Arctic. These cities with populations ranging from 50,000 to nearly 300,000 span four countries and three bioclimatic zones in northern Fennoscandia. They include coastal and inland cities—and have complex local geography associated with topography and water bodies. We analyze land surface temperature (LST) satellite remote-sensing data with the Moderate Resolution Imaging Spectroradiometer (MODIS) from 2000 to 2020. The aim is to assess the intensity and temporal (seasonal and interannual) variability and trends of LST anomalies to learn about surface UHI development over different time frames in the urban Arctic. We observed persistent urban temperature anomalies in every season in the range of 1–5 °C, with the highest values for the largest city Murmansk (Russia). There is a strong inverse relationship between surface UHI intensity and its temporal variability: the more substantial the surface UHI, the more stable it is and the lower its temporal variability. Murmansk and Tromsø (Norway) have the highest thermal anomalies showing relatively low temporal variability, whereas the surface UHI in Bodø (Norway) is low and very volatile. We found no general direction of surface UHI change in the long term, as statistically significant changes were identified for only 10 of 56 cases. The study also suggests that in addition to the size (population) of the city, the presence of compact and dense urban infrastructure causes strong and stable urban temperature anomalies and has a more significant impact than the geographical setting of the city.

1. Introduction

The increased development in urban areas has resulted in landscape morphology and surface changes and increased anthropogenic heat released into the atmosphere. Such changes lead to higher temperatures in urban areas than in the surrounding rural or suburban areas, forming heat islands. The most significant indicator of the intensity of a heat island is the temperature difference between the city and its rural surroundings. The urban heat island (UHI) is a widely used concept that quantifies this warming effect. In addition, urban construction often involves removing vegetation, soil, and depressions from the land surface, and changes in the local hydrology. All of this increases the vulnerability of cities to meteorological hazards and climate change. Ignoring the phenomenon of

* Corresponding author.

E-mail address: victoria.miles@nersc.no (V. Miles).

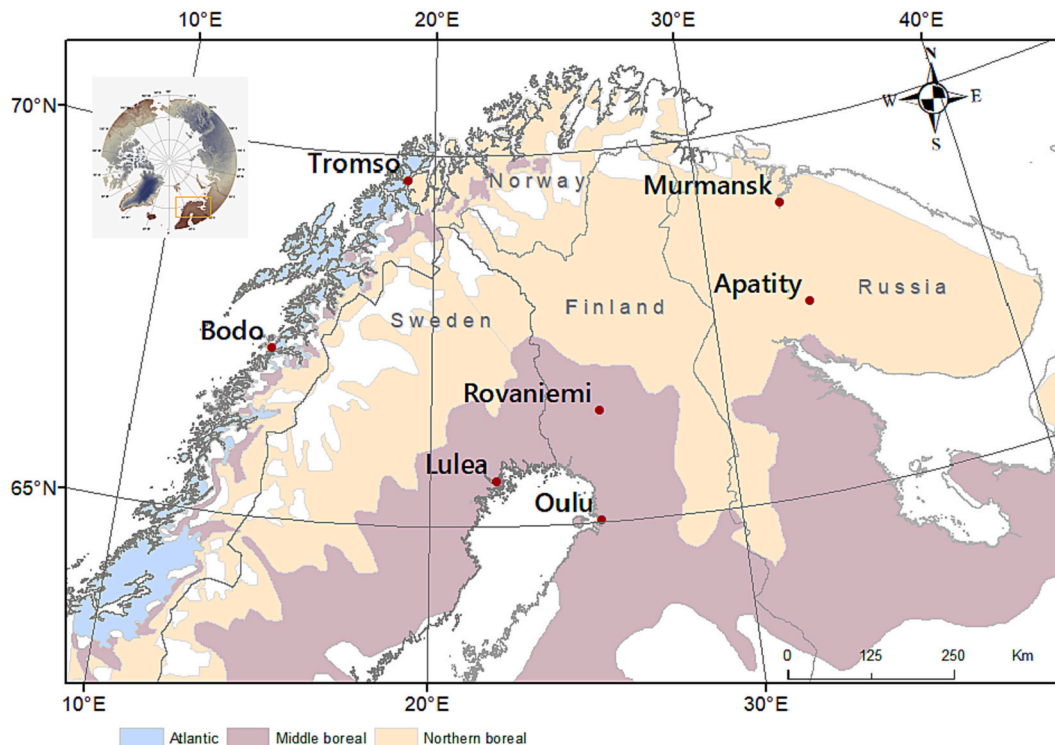


Fig. 1. The location of the seven cities with a population of >50,000 selected for the study—cities located in three bioclimatic zones and four different countries.

local urban climate in urban planning, water management, engineering, and energy can lead to disasters associated with damage to infrastructure and threats to human lives.

Several recent studies have found intense and persistent high-temperature anomalies associated with urban areas in high northern latitudes (e.g., Miles and Esau, 2017 and 2020). These results suggest that urban and suburban areas maintain additional heat, which accumulates from year to year, thereby creating a cumulative UHI effect in which a series of repetitive actions has an effect more than the sum of their individual effects. As shown by previous research, the cumulative UHI effect makes fundamental changes in the environment and soil properties, making them warmer and drier, and increases vegetation productivity, and enhancing the length of the growing season (Zhang et al., 2004; Alberti and Marzluff, 2004; Esau et al., 2016).

The UHI is developing in the background of global warming in the Arctic, which is greatly amplified in the Arctic compared to the lower latitudes (Alcoforado and Andrade, 2008; Serreze and Barry, 2011; Cohen et al., 2012). The observed UHI in the Arctic cities co-located with the expected future Arctic background temperature anomalies shows that many of these cities already have the temperature of the “future” (Esau et al., 2020) and thus can be used as models for changes in the rest of the Arctic over the next 30–50 years. Understanding the environmental impact of the warmer urban climate would help to assess and mitigate the regional warming processes (Monier et al., 2013). Urbanization is a continuing trend in the Arctic, and by mid-century, urban dwellers will account for >80% of the population of the Arctic. Northern Fennoscandia in the European Arctic is one of the most highly populated areas in the Arctic. Because the UHI scales with the urban size (Magee et al., 1999; Zhao et al., 2014), it is reasonable to expect more profound environmental changes around larger urbanized areas (Groisman and Gutman, 2013).

Here we present the first spatially and temporally comprehensive study of UHIs in the largest cities in the European Arctic, focusing attention on this understudied region. We leverage data and expand upon our previous study (Miles and Esau, 2020) to determine the intensity and variability of UHIs in all four seasons and daytime versus nighttime, 2000–2020. We use satellite remote-sensing data products to study urban thermal anomalies, specifically land surface temperature (LST) data obtained from the Moderate Resolution Imaging Spectroradiometer (MODIS). Due to high spatial and temporal resolution, MODIS LST data are often used to study UHIs (e.g., Gluch et al., 2006; Pu et al., 2006; Clinton and Gong, 2013; Miles and Esau, 2020). UHI measured by remote sensing data is called surface UHI. Yang et al. (2017) demonstrated that the averaged LST correlates well with the 2-m surface air temperature in the high northern latitudes. The analysis uses the database that includes LST from MOD11A2 collection 6 of Terra-MODIS. We analyze these LST data to quantify surface UHI intensity and its variability diurnally (daytime/nighttime), seasonally (summer, autumn, winter, and spring), and interannually from 2000 to 2020. We also estimate and assess trends in surface UHI intensity during the period. We then interpret the results with respect to the city size (population) and the regional and local geography.

The nature of urban heat anomalies is mainly due to anthropogenic factors. However, regional geography (e.g., macroclimate) and local geography can affect urban climate (due to topography, water bodies, and other features. Under such local conditions, the city-

induced heat and water fluxes to the lower atmosphere interact much more with the local air flows to create city-specific urban climates (Masson et al., 2020). Here we evaluate these factors in a case study of seven cities, each unique combination of climate, geography, and internal structure. For example, we have coastal (Murmansk, Tromsø, Oulu, Luleå and Bodø), inland (Rovaniemi), and mountainous (Apatity) cities located in three bioclimatic zones: Atlantic, middle boreal, and northern boreal.

2. Study area, data, and methods

2.1. Cities and background environment

Northern Fennoscandia is one of the highly populated areas in the Arctic and contains the largest cities in the European Arctic ($>65^{\circ}\text{N}$). The seven most significant cities in the European Arctic were selected for this analysis, and their locations are indicated in Fig. 1. (Severomorsk and Archangelsk in northwestern Russia are not included because of the former's proximity to the larger Murmansk, and the latter's location below 65°N .) These seven cities are in three different bioclimatic zones based on Moen et al.'s (1999) classification, and the climatology of these cities based on Köppen-Geiger (Peel et al., 2007), is listed in Table 1.

Bodø and Tromsø (Norway) are in the Atlantic coastal humid region. The most typical climatic feature of the Atlantic coastal regions is that the amplitude between the mean temperature of the coldest and warmest months is relatively small. The region receives high precipitation in all seasons. Bodø has a subpolar oceanic climate (Köppen-Geiger “Cfc”) / oceanic climate (“Cfb”), despite its northerly location on the Arctic Circle, thus representing a large anomaly from the zonal temperature. Bodø is located on a peninsula, and the most significant fraction of the urban surroundings is the ocean (Fig. 2). Tromsø has a subpolar oceanic climate (“Cfc”) / subarctic climate (“Dfc”). Tromsø is located on an island surrounded by an ice-free narrow fjord. Ocean, tundra, and forests are the three primary and nearly equal landcover classes in the urban-rural area (Fig. 2). Mountain slopes around the fjord are rather steep; they frequently lock a shallow mixed boundary layer over the city, creating proper conditions for aggravation of heat, moisture, and chemical air pollution. Although Tromsø has been included in a twin climate cities program – an exploratory study of future climate analogs for urban adaptation (Rohat et al., 2017) – there have been no formal urban climate studies of Tromsø.

Rovaniemi and Oulu (Finland), and Luleå (Sweden) are in the Middle boreal zone and have subarctic continental climates (Köppen-Geiger: “Dfc”). Middle boreal climates here typically feature a mean summer temperature of about 15°C , winter temperature of -8°C , and precipitation usually not higher than 500 mm. Due to its location near the Arctic Circle, these cities have short, moderate summers, while the winters are long, cold, and snowy. Rovaniemi is the second largest city in northern Finland and has an inland location just below the Arctic Circle. Oulu is the largest city in northern Finland and is situated by the Gulf of Bothnia, at the mouth of the Oulu River. Luleå is a coastal city in northern Sweden situated by the Gulf of Bothnia. Rovaniemi, Oulu and Luleå are to a large degree (nearly 50%) surrounded by forest landcover (Fig. 2).

Table 1

Geographical and climatic characteristics of seven studied cities in northern Fennoscandia. NB-northern boreal, MB-middle boreal, A-Atlantic. Dfc-boreal continental; Dfb-humid continental; Cfb-oceanic; Cfc-subpolar oceanic climate. Surface air temperature-SAT; Precipitation-PP.

City	Lat	Long	Elevation (m)	Population (000 s)	Urban area sq.km	Bioclim. zone	Climate class	Mean SAT ($^{\circ}\text{C}$)	Mean PP mm
Murmansk	68.979	33.092	53	296	52	NB	Dfc	0.2	481
Oulu	65.017	25.467	9	204	107	MB	Dfc	4	769
Luleå	65.583	22.150	12	767	25	MB	Dfc/Dfb	1.4	494
Tromsø	69.667	18.967	68	76	30	A	Dfc/Cfc	2.2	911
Rovaniemi	66.500	25.717	113	63	18	MB	Dfc	0.5	512
Apatity	67.564	33.403	172	56	23	NB	Dfc	-1	563
Bodø	67.283	14.383	22	52	10	A	Cfb/Cfc	4.5	981

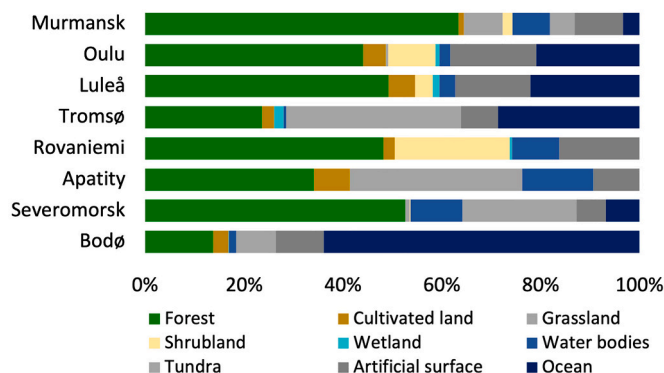


Fig. 2. Land cover types and their fraction, as a percent from the total area in the urban-rural areas, based on ESA CCI land cover map.

Murmansk and Apatity (Russia) are in the northern boreal zone and have subarctic continental climates (Köppen-Geiger: “Dfc”). Both cities are located on the Kola peninsula. The mean temperature in summer is $\sim 12^{\circ}\text{C}$ and winter is $\sim -16^{\circ}\text{C}$, and the amount of precipitation is < 450 mm. Murmansk is located on the eastern shore of the Kola Bay of the Barents Sea. The city's population is nearly 300,000, and it is the largest city in the Arctic. Murmansk's urban area has extreme elevation differences, with the highest point 306 m, and the lowest point is the coast of Kola Bay, which is at sea level. The city is also relatively green; the mean NDVI is 0.7. Forests occupy 43% of the urban area and $> 60\%$ of the rural area (Fig. 2). Apatity is a mid-size city in the interior of the Kola peninsula, and together with Rovaniemi, they both have more continental climates than other selected cities. The city occupies the top of a hill, lower ground near the lake Imandra. The climate of Murmansk and Apatity is better studied (Yakovlev, 1972; Demin et al., 2017; Varentsov et al., 2018; Konstantinov et al., 2014, 2015, 2018) than any other Arctic city, although those studies remain disconnected and highly fragmented.

2.2. Data and methods

2.2.1. MODIS LST climatology

In the study, we used the LST and emissivity product from MOD11A2 collection 6 of Terra-MODIS. The MOD11A2 product provides the LST in 8-day composites with relevant metadata, including quality assessment (Q.A.) information. The theoretical background and more detailed technical information about LST retrieval algorithm are thoroughly described in specialized publications such as Dash et al. (2002), Tomlinson et al. (2011), Hachem et al. (2012), Clinton and Gong (2013), and Hu and Brunsell (2015). LST composites were downloaded from NASA EarthData (<https://search.earthdata.nasa.gov>). The data were re-projected from the sinusoidal projection to the Universal Transverse Mercator (UTM) zone 33_N projection system with the WGS84 datum, reformatted from HDF-EOS to GeoTIFF format. In addition, they are converted from $^{\circ}\text{K}$ to $^{\circ}\text{C}$. The details of data processing steps are presented in detail in our previous publications (e.g., Miles and Esau, 2020).

In this study, we use seasonally averaged data for winter (December, January, February), spring (March, April, May), summer (June, July, August) and autumn (September, October, November), and daytime and nighttime periods for between 2000 and 2020. For Terra-MODIS, the satellite overpass times are approximately 10:30 and 22:30 local times. The average seasonal daytime and nighttime LST values per pixel were computed by aggregating the 8-day composites. As a result, we produced twelve LST maps for each year, i.e., day, night, and daily mean for each of the four seasons from 2000 to 2020.

2.2.2. Calculating urban temperature anomalies

The classical indicator to describe an surface UHI is the difference between urban and rural surface temperatures. Several other indicators have been suggested in the literature (e.g., Schwarz et al., 2011); however, in this study, we based on the classic theory described by Oke (1973, 1982, 1995). We calculate the surface UHI intensity as the difference between the maximum LST of the city cluster and the mean LST of land outside the city (buffer) (Miles, 2020; Esau et al., 2021). According to Oke, the urban area appears as a “plateau” of warm air with an increasing temperature towards the city center. The uniformity of the plateau is interrupted by the influence of distinct intra-urban land-uses such as parks, lakes, and open areas (cool), and commercial, industrial, or dense building areas (warm). The urban core shows a final ‘peak’ to the heat island where the maximum urban temperature is found. The difference between this value and the rural background temperature defines the surface UHI intensity (ΔT_{u-r}). A similar definition of the surface UHI intensity is found in Schwarz et al. (2011).

Urban pixels were allocated by city polygon; we considered rural to be the surrounding, non-urban land in a 5 km buffer. Analogously, T_r denotes the boundary temperature, considered as a measure for the background temperature. The resulting ΔT value represents the difference between the maximum temperature of the city cluster (T_u) and the mean temperature of land outside the city (T_r):

$$\Delta T = T_u - T_r$$

Zonal statistics extracted thematic information for different vector data: bioclimatic zone, rural area, and urban area. The ArcGIS software has been used to processed and analyzed (more details in Miles, 2020; Miles and Esau, 2020; Esau et al., 2021). The set of extracted variables is presented in Table 1.

2.2.3. Calculation of the interannual, seasonal, and diurnal changes

In addition, the mean values \bar{x} and standard deviations (SD) were calculated for the LSTs and surface UHI in each area and period. To measure the interannual variability of surface UHIs relative to their mean magnitude, the coefficient of variation (CV) was calculated on an annual basis by considering the seasonal and day/night temperature values of the year. Thus, the CV was determined as the ratio of standard deviation to mean.

$$CV = \frac{SD}{\bar{x}} * 100$$

Linear trend analysis was conducted to calculate the rates of temporal change. We calculated the trend for the urban LST, rural (buffer) LST, and surface UHI. First, we identify the cities and seasons with statistically significant ($p < 0.05$) trends in surface UHI. For all cases, we examine the urban and rural temperature trends for insight into the surface UHI trends (or lack thereof). Then, for the significant cases, we calculate the surface UHI trend through regression equation ($y = \text{UHI}$, $x = \text{year}$), expressed as $^{\circ}\text{C}$ per decade.

3. Results

3.1. SUHI intensity and its seasonal and diurnal variability

Analysis of LST data identified consistently higher surface temperatures in urban areas than in rural background areas. Persistent anomalies are observed annually for 21 years in every season. However, the surface UHI intensity and its seasonal and diurnal variability vary from city to city (Table 2, Fig. 3). The highest contrast between urban and rural LSTs was found in Murmansk, the largest city. In Murmansk, we observed warm urban anomalies higher than in other cities every year and season. The highest average surface UHI value (5.5 °C) is observed in winter, and in some years, the urban areas can be 8 °C warmer than the surrounding landscapes. The second highest surface UHI values are observed in Tromsø, especially in winter and spring, when the urban LST anomaly is 4.7–5.1 °C higher than the surrounding areas. Finally, a little contrast between urban and rural LST was found for Bodø (Table 2, Fig. 3a).

Daytime urban temperature anomalies are generally more substantial than nighttime (Fig. 3a,c). In Tromsø, surface UHI is more intense during the daytime in autumn, winter, and spring but almost equal in summer. In Oulu, Luleå, Rovaniemi, Apatity, and Bodø, urban summer daytime temperature anomalies are 30–50% higher than at other times of the year. Murmansk is the only city where the

Table 2

Surface UHI intensity (°C) and its variability for the seven case cities, stratified by season and daytime vs. nighttime. Intra-annual variability is indicated by the seasonal and diurnal breakdown of the mean UHI intensity (mean ΔT) – see Section 3.1. Interannual variability is indicated by the minimum (min ΔT), maximum (max ΔT), standard deviation (SD ΔT) and coefficient of variation (CV) of the UHI – see Section 3.2.

City	Summer day (SD)					Summer night (SN)				
	Mean ΔT	Min ΔT	Max ΔT	SD ΔT	CV	Mean ΔT	Min ΔT	Max ΔT	SD ΔT	CV
Murmansk	3.2	2.2	4.6	0.50	16%	4.2	2.9	6.8	0.78	19%
Oulu	4.0	3.3	4.9	0.45	11%	2.9	2.2	7.1	1.04	36%
Lulea	3.5	2.6	6.3	0.79	22%	2.4	1.7	6.1	1.02	43%
Tromsø	2.7	1.2	5.1	1.03	39%	2.5	1.8	4.0	0.55	22%
Rovaniemi	2.7	2.0	3.8	0.53	19%	1.6	0.8	2.2	0.39	24%
Apatity	3.7	2.8	4.8	0.55	15%	1.8	0.9	2.4	0.36	20%
Bodø	2.4	1.0	4.4	0.69	29%	0.7	−0.1	2.3	0.54	80%

City	Autumn day (AD)					Autumn night (AN)				
	Mean ΔT	Min ΔT	Max ΔT	SD ΔT	CV	Mean ΔT	Min ΔT	Max ΔT	SD ΔT	CV
Murmansk	3.9	2.8	5.8	0.87	22%	4.2	2.7	6.0	0.87	21%
Oulu	2.5	1.4	4.9	0.90	36%	3.2	1.4	5.1	0.90	28%
Lulea	2.1	0.9	4.1	0.96	47%	1.9	0.6	3.7	0.96	51%
Tromsø	3.4	1.8	5.1	0.93	28%	2.3	0.6	3.7	0.93	40%
Rovaniemi	2.0	0.1	3.8	0.98	49%	1.9	1.2	3.7	0.98	50%
Apatity	1.2	0.5	2.4	0.54	43%	0.7	−0.2	1.3	0.54	74%
Bodø	0.7	0.0	1.6	0.46	66%	0.4	−0.4	1.4	0.46	109%

City	Winter day (WD)					Winter night (WN)				
	Mean ΔT	Min ΔT	Max ΔT	SD ΔT	CV	Mean ΔT	Min ΔT	Max ΔT	SD ΔT	CV
Murmansk	5.5	4.6	6.8	0.57	10%	5.2	3.9	6.6	0.71	14%
Oulu	2.8	1.5	3.6	0.65	23%	3.0	1.6	4.9	0.79	26%
Lulea	2.1	0.5	4.3	0.92	44%	2.3	0.5	5.0	0.99	43%
Tromsø	4.7	3.1	6.1	0.72	15%	3.7	1.9	4.9	0.74	20%
Rovaniemi	1.2	−0.1	3.0	0.72	61%	1.5	0.4	2.6	0.55	37%
Apatity	0.9	0.3	2.1	0.46	54%	1.1	0.1	2.1	0.50	46%
Bodø	1.7	0.7	2.8	0.71	42%	1.1	−0.4	3.0	0.80	74%

City	Spring day (SprD)					Spring night (SprN)				
	Mean ΔT	Min ΔT	Max ΔT	SD ΔT	CV	Mean ΔT	Min ΔT	Max ΔT	SD ΔT	CV
Murmansk	4.5	1.7	6.0	0.87	19%	4.4	0.3	5.8	0.87	20%
Oulu	2.8	0.1	4.6	0.90	32%	2.4	0.2	4.1	0.90	38%
Lulea	2.0	0.3	3.0	0.96	47%	1.5	−0.6	4.4	0.96	63%
Tromsø	4.9	0.4	8.4	0.93	19%	2.8	−1.2	4.4	0.93	33%
Rovaniemi	1.8	0.0	2.9	0.98	53%	1.7	−1.2	3.6	0.98	59%
Apatity	2.0	1.2	3.1	0.54	27%	1.4	−0.2	2.0	0.54	39%
Bodø	1.8	−0.6	3.9	0.46	26%	0.7	−4.7	2.4	0.46	65%

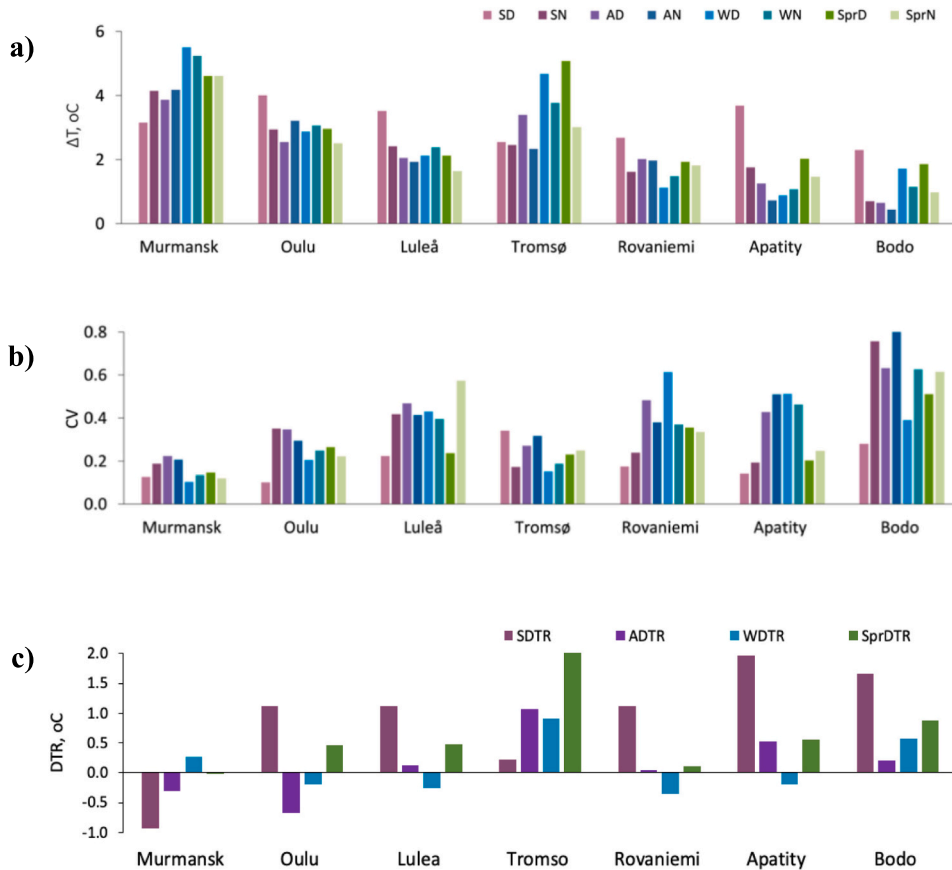


Fig. 3. Surface UHI characteristics for the seven case cities, stratified by season and daytime/nighttime: summer day (SD), summer night (SN), autumn day (AD), autumn night (AN), winter day (WD), winter night (WN), spring day (SprD) and spring night (SprN). (a) Surface UHI seasonal and diurnal variability. The plotted values are those shown in bold in Table 2. (b) Interannual variability of surface UHI relative to the mean, as indicated by the coefficient of variation (CV). (c) Difference between daytime and nighttime UHI in the four different seasons, expressed as the diurnal temperature range (DTR). Positive values indicate a stronger UHI in daytime, and negative values indicate a stronger UHI in nighttime.

summer surface UHI is higher at night than during the day (4.1° versus 3.2 °C). Fig. 4 shows an example of summer nighttime surface UHI in Murmansk. Urban LST contrasts strongly with cooler suburban/rural areas; the actual (not averaged) LST difference can be up to 6 °C. Most cities show overall surface UHI stability and low variability over 21 years during summer daytime, as evidenced by low CV values averaging ~20% (Table 2).

3.2. Interannual variability of surface UHI

The year-to-year variability of surface UHI intensity is different from city to city and depends on the season and daytime/nighttime. Figs. 3b and 5 illustrate the surface UHI intensity's interannual variability from 2000 to 2020. Bodø, Rovaniemi, and Apatity have relatively weak surface UHI intensity with high volatility from year to year and between seasons, whereas Murmansk and Tromsø have the highest thermal anomalies showing relatively low temporal variability.

Thus there is a clear inverse relationship between surface UHI intensity and its temporal variability: the stronger the surface UHI, the more stable it is and the lower its temporal variability on interannual time scales (Fig. 6). The correlation between surface UHI and its coefficient of variation is strong ($r \sim -0.78$) and statistically significant ($P < 0.001$) (Fig. 6b).

3.3. Trends in surface UHI

Trend analysis identified statistically significant changes for only 10 of 56 cases (Table 3). Moreover, no general direction of surface UHI trends was identified, e.g., in spring and summer, both positive and negative trends were observed, and in autumn and winter, the trends were only negative. No significant trends were identified during spring nights or autumn days.

Negative winter nighttime surface UHI trends in Tromsø and Murmansk have happened in the background of near-neutral or negative LST change in an urban area, while a positive trend was observed in rural areas. In Bodø, a significant negative surface UHI

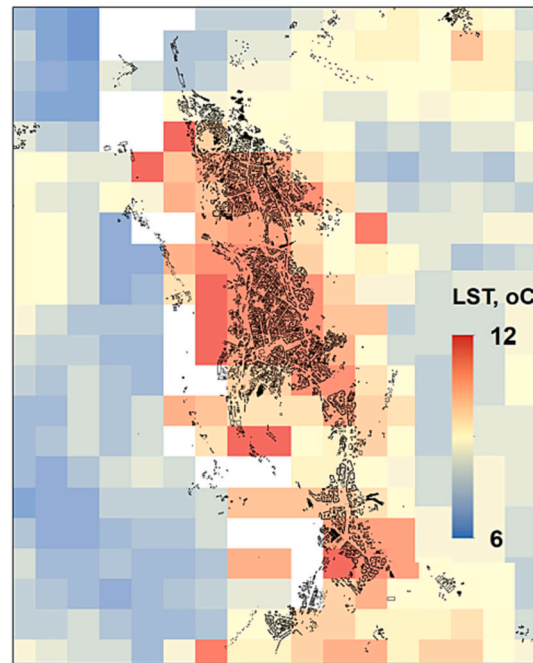


Fig. 4. Example of summer night LST distribution in Murmansk and surrounding areas.

trend during the winter daytime, with a positive background temperature trend in rural areas. For Rovaniemi and Oulu marked positive trends during the summer daytime. The increase was impacted by the higher positive trend in urban temperatures than in rural areas.

In contrast, a negative trend in Bodø in summer nighttime was on near-neutral change in urban temperature increasing rural temperature. No significant surface UHI trends were identified during the autumn daytime. However, a negative trend at night was observed in Apatity and Oulu due to decreased temperature in rural areas. At the same time, it was close to a neutral or slightly increasing trend in cities. The positive trend on a spring day was identified in Rovaniemi as a positive urban trend and a negative rural trend. On the other hand, the negative trend for Murmansk is due to near-neutral urban temperatures while rural temperatures slightly increased.

4. Discussion

In the study, we analyzed the temporal variability and trends of urban LST anomalies in the seven most prominent cities of the European Arctic. Analysis of MODIS LST data for 21 years shows that UHI prevails in most cases in all seven cities, both seasonally and annually.

The most substantial urban temperature anomalies are observed in the two largest coastal cities - Murmansk and Tromsø. Their urban areas can heat up significantly, especially in winter, when stable atmospheric stratification and low boundary layers help trap heat in urban areas (Esau et al., 2012). Research shows that the general surface UHI behaviour in northern cities differs from that in mid and low latitudes (Konstantinov et al., 2014, 2015; Brozovsky et al., 2021). The difference appears in seasonal and diurnal cycles. The principal confirmed difference is that the winter surface UHI is higher in northern cities (Miles and Esau, 2017; Suomi, 2018; Miles and Esau, 2020). The second significant difference is that the typical summer surface UHI for high latitude cities is more potent during the day than at night (Miles and Esau, 2020). Therefore, in contrast to the commonly accepted surface UHI seasonality in a temperate climate, here the winter surface UHI of these two cold climate cities is stronger than the summer surface UHI. In some years, we found that the intensity can be two degrees higher than the average for Murmansk. After comparison with data from the meteorological station in Murmansk (Kivinen et al., 2017), we discovered that the high winter surface UHI corresponds with cold extremes. The intense urban heat anomalies during colder climatic conditions were discovered by Varentsov et al. (2018). The results of field measurements of urban heat islands in seven Russian Arctic cities confirm that surface UHI intensity increases in colder conditions (Konstantinov et al., 2018). The released anthropogenic heat remains in a shallow surface layer during cold atmospheric conditions where the atmospheric stability impedes the vertical mixing. Therefore, even relatively modest heat fluxes can significantly raise temperatures (Esau et al., 2012; Davy and Esau, 2014, 2016). This mechanism gives an amplifying factor to the surface UHI in mid-sized arctic cities. Even though arctic winters are becoming warmer (Graham et al., 2017), the number of cold extremes is increasing (Johnson et al., 2018; Koenigk et al., 2019).

Here, we find that cities with high surface UHI intensity exhibit low temporal variability and indicates the presence of a permanent surface UHI. For example, the winter UHI in Murmansk is the strongest and has generally <20% interannual variability. On the other

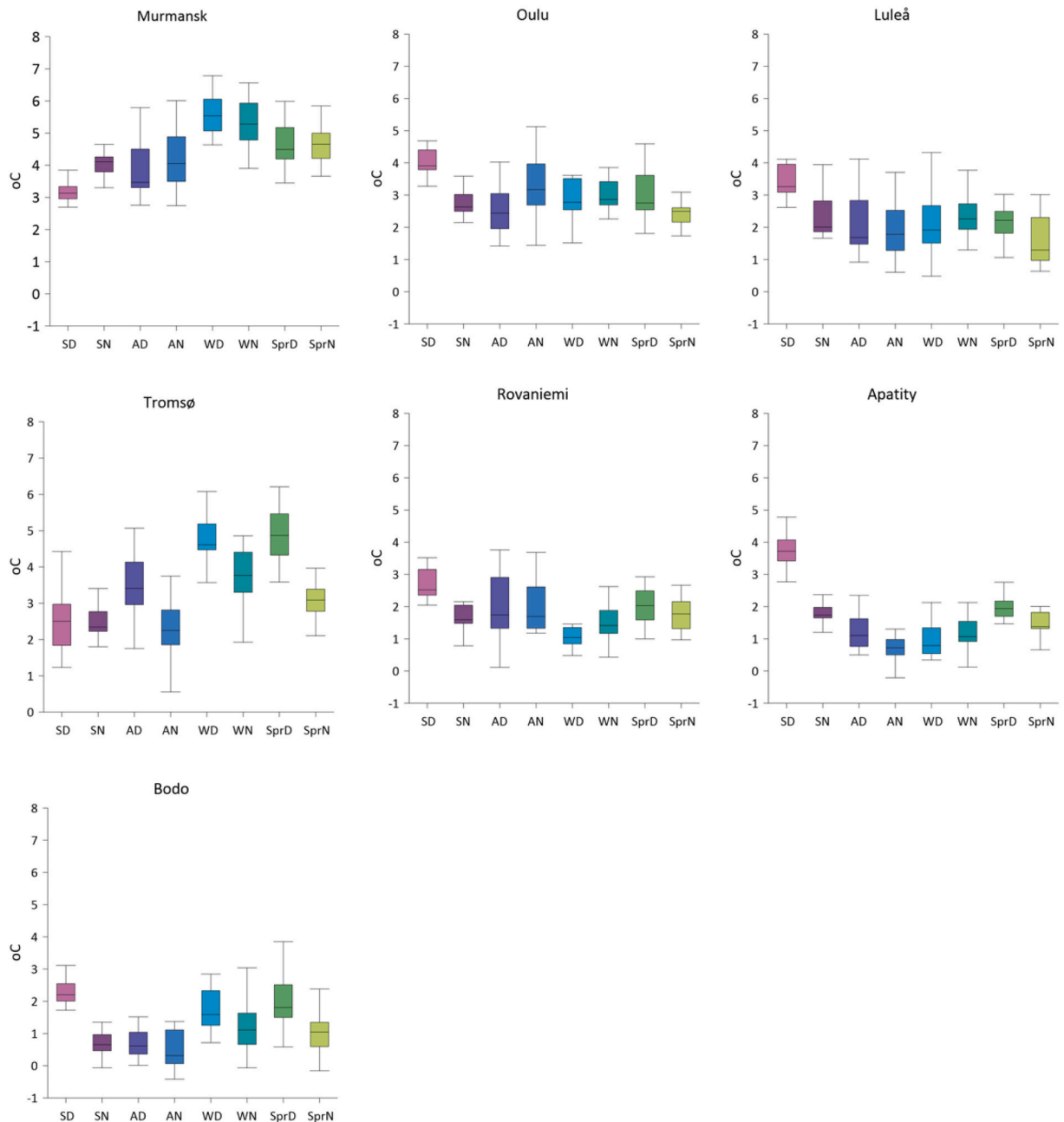


Fig. 5. Diurnal, seasonal and interannual variability of surface UHI for the seven case cities in the period 2000–2020. Box and whiskers plots show the median, range and quartile variability in the period 2000–2020.

hand, the weakest winter UHI in Bodø has nearly 80% interannual variability. Surface UHI stability means that part of the “urban factory” has a constant heat accumulation or production source. Thus, for example, persistent solid winter heat anomalies were observed in the northwest Siberian city of Surgut, which has a vital source of anthropogenic heat emission (Miles and Esau, 2017).

Murmansk exhibits a strong night-time summer surface UHI, similar to cities in the middle and low latitudes. Murmansk is a large city with a well-allocated dense city center. It is the greenest of all studied cities, with a mean urban NDVI is 0.7. Forests occupy 63% of the urban buffer and provide a contrasting cooling effect. Previous studies of Arctic cities (Miles and Esau, 2017, 2020) observed more prominent summer day surface UHI than night-time. The proposed reasons for that were: 1) insufficient solar heating to provide the required amount of heat to be accumulated and released at night-time; 2) a small area of the city and insufficiently dense urban structures and 3) a small amount of vegetation in rural areas and not sufficient evaporation to provide the needed cooling effect in the rural areas. Therefore, in Murmansk, we find opposite conditions, similar to surface UHI formation in lower latitude cities.

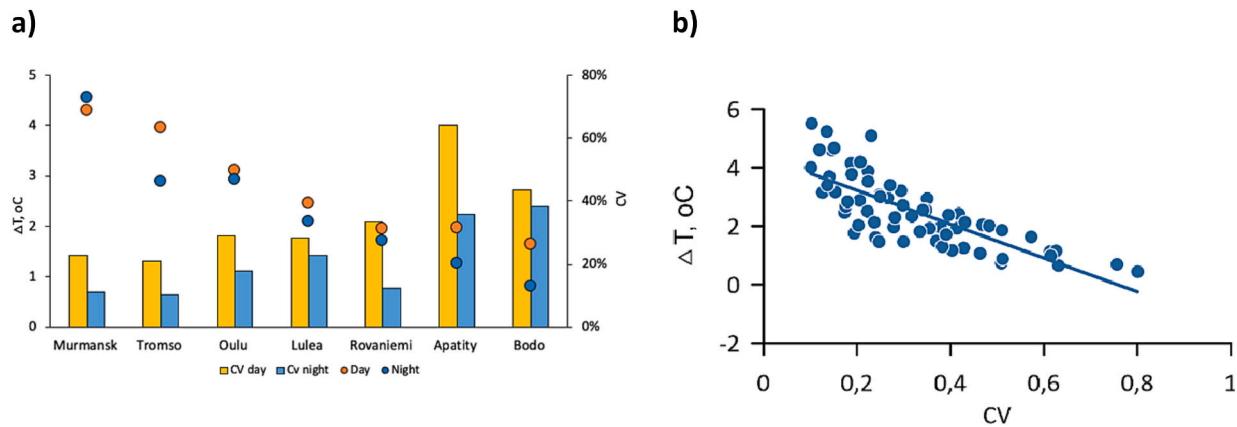


Fig. 6. (a) Surface UHI strength versus interannual variability for each city, stratified by daytime versus nighttime. Circles are mean annual value (ΔT °C) and bars are the coefficient of variation (CV). (b) Relationship between mean surface UHI and its interannual variation ($r = 0.78$; $P < 0.001$) for all cities, seasons, and daytime/nighttime ($n = 56$).

Luleå and Oulu have the most stable surface UHIs both day and night at any time of the year. Surface UHI summer day was stronger for Rovaniemi and Apatity. We compare cities based on the variability of the surface UHI intensity at different times of the year. The city of Bodø shows a unique behaviour. Bodø is the smallest city and has a strong ocean impact due to its location on a peninsula, showing the weakest and most unstable surface UHI.

We found general positive LST trends for urban and rural background areas. For example, Fig. 7 shows an average increase in summer LST for all urban and rural areas. We observe nearly synchronous annual variability in both rural and urban areas. However, individually cities show their own unique behaviour. The direction of surface UHI change can be opposite to the direction of the background trend. For example, significant decreases in UHI magnitude in winter for Tromsø, Murmansk, and Bodø are evident against the positive trend in a rural background and near neutral or slightly negative urban LST trend.

In contrast, the increased surface UHI effect for Rovaniemi and Oulu results from a more significant positive trend in urban temperature than for rural temperature. Inland cities show significant positive trends in winter, summer, and spring, while coastal towns show negative trends in the same seasons. Apatity, the only mountain town in our study, has a solid negative autumn trend, while there was no trend for the other seasons. The positive correlation with urban LSTs and a negative with rural LSTs indicates that the variation in surface UHI intensity is determined mainly by the variability of the city's temperatures (Fig. 8). For Murmansk and Tromsø, we observed a general decreasing urban–rural difference, i.e., a negative trend in surface UHI. This is due to increased rural

Table 3
Statistically significant ($p = 0.05$) trends in UHI, in degrees C per decade.

City	Summer		Autumn		Winter		Spring	
	Day	Night	Day	Night	Day	Night	Day	Night
Murmansk						−0.65	−0.74	
Oulu	0.34			−0.65				
Luleå								
Tromsø						−0.75		
Rovaniemi	0.4						0.48	
Apatity			−1.09					
Bodø		−0.49						

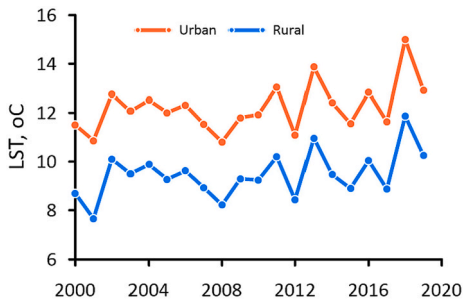


Fig. 7. Average for all seven cities' summer LST, urban and rural.

	Sd	Sn	Ad	An	Wd	Wn	sprD	sprN	
Urban	0.6	0.7	-0.12	0.26	0.02	-0.12	-0.44	-0.26	Murmansk
	0.7	0.7	0.02	0.11	-0.24	0.03	0.04	-0.52	Oulu
	0.5	0.6	0.27	0.26	0.12	0.51	0.37	0.08	Luleå
	0.6	0.4	-0.05	0.43	0.34	0.63	0.51	0.36	Tromsø
	0.5	0.4	0.47	0.42	0.00	0.22	0.19	0.14	Apatity
	0.4	0.6	-0.26	-0.13	0.29	0.54	0.30	0.04	Rovaniemi
	0.3	-0.1	0.33	0.36	0.16	0.53	0.00	0.25	Bodø
Rural	0.0	0.4	-0.52	-0.21	-0.32	-0.55	-0.73	-0.67	Murmansk
	0.3	0.3	-0.37	-0.34	-0.48	-0.26	-0.36	-0.71	Oulu
	-0.1	0.2	-0.24	-0.09	-0.31	0.17	0.08	-0.36	Luleå
	-0.3	-0.3	-0.61	-0.15	-0.44	-0.33	-0.30	-0.28	Tromsø
	0.1	0.4	-0.58	-0.50	-0.06	0.36	-0.04	-0.34	Rovaniemi
	-0.1	0.0	0.26	0.20	-0.25	-0.04	-0.03	-0.13	Apatity
	-0.3	-0.4	0.01	-0.04	-0.51	-0.19	-0.47	-0.53	Bodø

Fig. 8. Correlation between surface urban heat island (SUHI) and urban and rural temperature. Color shading indicates the relative strength of positive (red) and negative (blue) correlations.

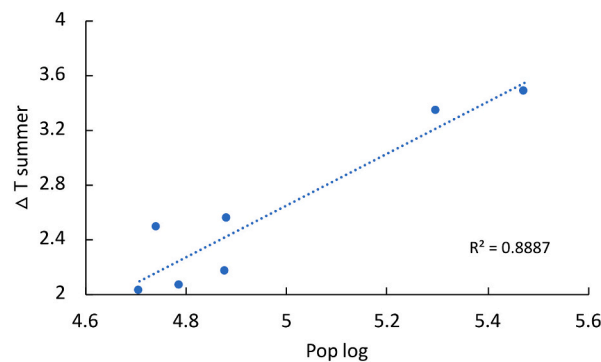


Fig. 9. Relationship between summer surface urban heat island intensity and logarithm of urban population. Linear regression for logarithm of population yields an $R^2 = 0.89$ ($P \leq 0.05$).

temperature and near neutral or slightly negative urban LST trend. The substantial increase of urban LST was typical for inland cities in summer and spring. And the second case is with decreasing urban LST and increasing rural background LST for the coastal towns in winter. We observe the increase of surface UHI in stable low wind climatic conditions during cold winter or warm summer climatic extremes. This issue needs further investigation.

Correlation analysis of UHI intensity with different local parameters such as percent of vegetation, vegetation index, water fraction and urban population found that population has the highest influential factor on summer surface UHI (Fig. 9), a statistically significant result despite having a very small sample of cases ($n = 7$).

5. Conclusions

This study documents the existence and characteristics of the surface urban heat island (SUHI) in the seven largest cities in the European Arctic. Analysis of the mean and variability stratified by season and day versus night identified heterogeneity in surface UHI characteristics amongst the cities, which have different sizes and background environments. The main findings are as follows:

1. There are persistent urban temperature anomalies (surface UHIs) in every season in the range of 1–5 °C in each of the studied cities. The highest value is 5.5 °C during the winter nighttime in the largest city Murmansk. City size (population) is the factor with the highest correlation with surface UHI intensity.

2. There is a clear inverse relationship between surface UHI intensity and its temporal variability: the stronger the surface UHI, the more stable it is and the lower its temporal variability on interannual time scales. The estimated correlation between UHI and its coefficient of variation is strong ($r \sim -0.78$). In particular, Murmansk and Tromsø (Norway) have the highest thermal anomalies showing relatively low temporal variability, whereas the surface UHI in Bodø (Norway) is low and very volatile.
3. Changes in surface UHI intensity mainly reflect the changes in urban temperature. But there is no significant common trend in surface UHI intensity discovered. However, there are two general situations: an increase of surface UHI on the background of negative rural and positive urban LST trends and a decrease of surface UHI on the rise in rural and neutral or negative urban LST. Thus, we see that the background warming trends do not associate with the intensity of surface UHI.
4. Surface UHI increased during cold and warm climatic extremes when developed special meteorological conditions that held the heat due to shallow boundary layers and low mixing.

We conclude that surface urban heat anomalies are an essential feature of the largest cities in the European Arctic in all seasons. The persistent presence of UHIs means that these urban areas are under constant pressure from accumulated heat and heat flow generated by urban metabolism. The warmer urban climate is a major concern for the urban economy, the environment, and human health. Mainly due to global climate change in the arctic and high mountain regions, the rate of warming is higher than in the rest of the world, and the urban environment has become a “hot spot” due to the UHI effect. Therefore, unpredictable consequences are possible if the UHI effect in urban planning and development is not considered. The current trend in Northern Europe is the densification of the urban center. Compaction affects urban microclimate, accelerates heat island effects, and forms sustainable urban heat islands.

Sample credit author statement

Victoria Miles: Conceptualization, Methodology, Data curation, Investigation, Visualization, Writing- Original draft preparation, Writing-review&editing. **Igor Ezau:** Conceptualization, Methodology, Writing- Original draft preparation. **Martin Miles:** Formal analysis, Methodology, Investigation, Writing- Original draft preparation, Writing-review&editing.

Data availability

No data was used for the research described in the article.

Acknowledgement

This study was supported by the Belmont Forum and the Norwegian Research Council's project “Increasing social and environmental sustainability through urban green, blue and white space” and the Nordic Center of Excellence project ARCPATH “Arctic Climate Predictions - Pathways to Resilient, Sustainable Societies”.

References

- Alberti, M., Marzluff, J., 2004. Resilience in urban ecosystems: linking urban patterns to human and ecological functions. *Urban Ecosyst.* 7, 241–265.
- Alcoforado, M.J., Andrade, H., 2008. Global warming and the urban heat island. In: *Urban Ecology*. Springer US, New York, NY, USA, pp. 249–262.
- Brozovsky, J., Gaitani, N., Gustavsen, A., 2021. A systematic review of urban climate research in cold and polar climate regions. *Renew. Sust. Energ. Rev.* 138 <https://doi.org/10.1016/j.rser.2020.110551>. Elsevier Ltd.
- Clinton, N., Gong, P., 2013. MODIS detected surface urban heat islands and sinks: global locations and controls. *Remote Sens. Environ.* 134, 294–304. <https://doi.org/10.1016/j.rse.2013.03.008>.
- Cohen, J.L., Furtado, J.C., Barlow, M.A., Alexeev, V.A., Cherry, J.E., 2012. Arctic warming, increasing snow cover and widespread boreal winter cooling. *Environ. Res. Lett.* 7 (1) <https://doi.org/10.1088/1748-9326/7/1/014007>.
- Dash, P., Götsche, F.M., Olesen, F.S., Fischer, H., 2002. Land surface temperature and emissivity estimation from passive sensor data: theory and practice – current trends. *Int. J. Rem. Sens.* 23, 2563–2594. <https://doi.org/10.1080/01431160110115041>.
- Davy, R., Esau, I., 2014. Global climate models' bias in surface temperature trends and variability. *Environ. Res. Lett.* 9, 114024. <https://doi.org/10.1088/1748-9326/9/11/114024>.
- Davy, R., Esau, I., 2016. Differences in the efficacy of climate forcings explained by variations in atmospheric boundary layer depth. *Nat. Commun.* 7, 11690. <https://doi.org/10.1038/ncomms11690>.
- Demin, V., Anziferova, A., Chaus, O., 2017. Influence of meteorological conditions on calculation of the urban heat island in Murmansk. *Proc. Hydrometeorol. Res. Center Russ. Feder.* 363, 160–175 (in Russian).
- Esau, I., Davy, R., Outten, S., 2012. Complementary explanation of temperature response in the lower atmosphere. *Environ. Res. Lett.* 7 (4), 044026 <https://doi.org/10.1088/1748-9326/7/4/044026>.
- Esau, I., Miles, V., Davy, R., Miles, M.W., Kurchatova, A., 2016. Trends in normalized difference vegetation index (NDVI) associated with urban development in northern West Siberia. *Atmos. Chem. Phys.* 16, 9563–9577. <https://doi.org/10.5194/acp-16-9563-2016>.
- Esau, I., Varentsov, M., Laruelle, M., Miles, M.W., Konstantinov, P., Soromotin, A., Baklanov, A.A., Miles, V.V., 2020. In: Pokrovsky, O., et al. (Eds.), *Warmer Climate of Arctic Cities, in monograph The Arctic: Current Issues and Challenges*. NOVA Publishers. ISBN: 978-1-53617-306-2. <https://novapublishers.com/shop/the-arctic-current-issues-and-challenges/>.
- Esau, I., Miles, V., Soromotin, A., Sizov, O., Varentsov, M., Konstantinov, P., 2021. Urban heat islands in the Arctic cities: an updated compilation of in situ and remote-sensing estimations. *Adv. Sci. Res.* 18, 51–57. <https://doi.org/10.5194/asr-18-51-2021>.
- Gluch, R., Quattrochi, D., Luval, J., 2006. A multi-scale approach to urban thermal analysis. *Remote Sens. Environ.* 104, 123–132. <https://doi.org/10.1016/j.rse.2006.01.025>.
- Graham, R.M., Cohen, L., Petty, A.A., Boisvert, L.N., Granskog, M.A., Rinke, A., Hudson, S.R., Nicolaus, M., 2017. Increasing frequency and duration of Arctic winter warming events. *Geophys. Res. Lett.* 44, 6974–6983. <https://doi.org/10.1002/2017GL073395>.
- Groisman, P., Gutman, G. (Eds.), 2013. *Environmental Changes in Siberia: Regional Changes and their Consequences*. Springer, Amsterdam.

- Hachem, S., Duguay, C.R., Allard, M., 2012. Comparison of MODIS derived land surface temperatures with ground surface and air temperature measurements in continuous permafrost terrain. *Cryosphere* 6, 51–69. <https://doi.org/10.5194/tc-6-51-2012>.
- Hu, L., Brunsell, N.A., 2015. A new perspective to assess the urban heat island through remotely sensed atmospheric profiles. *Remote Sens. Environ.* 158, 393–406. <https://doi.org/10.1016/j.rse.2014.10.022>.
- Johnson, N.C., Xie, S.P., Kosaka, Y., et al., 2018. Increasing occurrence of cold and warm extremes during the recent global warming slowdown. *Nat. Commun.* 9, 1724. <https://doi.org/10.1038/s41467-018-04040-y>.
- Kivinen, S., Rasmus, S., Jylhä, K., Laapas, M., 2017. Long-term climate trends and extreme events in Northern Fennoscandia (1914–2013). *Climate* 5 (1), 16. <https://doi.org/10.3390/cli5010016>.
- Koenigk, T., Gao, Y., Gastineau, G., et al., 2019. Impact of Arctic Sea ice variations on winter temperature anomalies in northern hemispheric land areas. *Clim. Dyn.* 52, 3111–3137. <https://doi.org/10.1007/s00382-018-4305-1>.
- Konstantinov, P., Baklanov, A., Varentsov, M., Kukanova, E., Repina, I., 2014. Experimental urban heat island research of four biggest polar cities in Northern Hemisphere. In: *Geophys. Res. Abst. EGU General Assembly*, 16, p. 10699.
- Konstantinov, P.I., Grishchenko, M.Y., Varentsov, M.I., 2015. Mapping urban heat islands of Arctic cities using combined data on field measurements and satellite images based on the example of the city of Apatity (Murmansk Oblast). *Izv. Atmos. Ocean Phys.* 51, 992–998. <https://doi.org/10.1134/S000143381509011X>.
- Konstantinov, P., Varentsov, M., Esau, I., 2018. A high density urban temperature network deployed in several cities of Eurasian Arctic. *Environ. Res. Lett.* 13, 75007. <https://doi.org/10.1088/1748-9326/aacb84>.
- Magee, N., Curtis, J., Wendler, G., 1999. The urban heat island effect at Fairbanks, Alaska. *Theor. Appl. Climatol.* 64, 39–47. <https://doi.org/10.1007/s007040050109>.
- Masson, V., Lemonsu, A., Hidalgo, J., Voogt, J., 2020. Urban climates and climate change. *Annu. Rev. Environ. Resour.* <https://doi.org/10.1146/annurev-environ-012320-083623>.
- Miles, V.V., 2020. Arctic Surface Urban Heat Island (UHI), MODIS Land Surface Temperature (LST) Data, 2000–2016. Arctic Data Center. <https://doi.org/10.18739/A2TB0XW4T>.
- Miles, V., Esau, I., 2017. Seasonal and spatial characteristics of Urban Heat Islands (UHI) in northern West Siberian cities. *Remote Sens.* 9, 989. <https://doi.org/10.3390/rs9100989>.
- Miles, V., Esau, I., 2020. Surface urban heat islands in 57 cities across different climates in northern Fennoscandia. *Urban Clim.* 31 <https://doi.org/10.1016/j.uclim.2019.100575>.
- Moen, A., Lillethun, A., Odland, A., 1999. *Vegetation, National Atlas of Norway*. Norwegian Mapping Authority. Hønefoss 200 s, ISBN: 8279450009 9788279450009.
- Monier, E., Sokolov, A., Schlosser, A., Scott, J., Gao, X., 2013. Probabilistic projections of 21st century climate change over northern Eurasia. *Environ. Res. Lett.* 8, 045008. <https://doi.org/10.1088/1748-9326/8/4/045008>.
- Oke, T.R., 1973. City size and the urban heat island. *Atmos. Environ.* 7, 769–779.
- Oke, T.R., 1982. The energetic basis of the urban heat-island. *Q. J. R. Meteorol. Soc.* 108, 1–24.
- Oke, T.R., 1995. The heat island characteristics of the urban boundary layer: Characteristics, causes and effects. In: Cermak, J.E., et al. (Eds.), *Wind Climate in Cities*. Kluwer Academic, pp. 81–107.
- Peel, M.C., Finlayson, B.L., McMahon, T.A., 2007. Updated world map of the Köppen-Geiger climate classification. *Hydrol. Earth Syst. Sci.* 11, 1633–1644. <https://doi.org/10.5194/hess-11-1633-2007>.
- Pu, R., Gong, P., Michishita, R., Sasagawa, T., 2006. Assessment of multi-resolution and multi-sensor data for urban surface temperature retrieval. *Remote Sens. Environ.* 104, 211–225. <https://doi.org/10.1016/j.rse.2005.09.022>.
- Rohat, G., Goyette, S., Flacke, J., 2017. Twin climate cities—an exploratory study of their potential use for awareness-raising and urban adaptation. *Mitig. Adapt. Strateg. Glob. Chang.* 22 (6), 929–945. <https://doi.org/10.1007/s11027-016-9708-x>.
- Schwarz, N., Lautenbach, S., Seppelt, R., 2011. Exploring indicators for quantifying surface urban heat islands of European cities with MODIS land surface temperatures. *Remote Sens. Environ.* 115, 3175–3186. <https://doi.org/10.1016/j.rse.2011.07.003>.
- Serreze, M.C., Barry, R.G., 2011. Processes and impacts of Arctic amplification: a research synthesis. *Glob. Planet. Chang.* 77, 85–96. <https://doi.org/10.1016/j.gloplacha.2011.03.004>.
- Suomi, J., 2018. Extreme temperature differences in the city of Lahti, southern Finland: intensity, seasonality, and environmental drivers. *Weather Clim. Extrem.* 19, 20–28. <https://doi.org/10.1016/j.wace.2017.12.001>.
- Tomlinson, C.J., Chapman, L., Thornes, J.E., Baker, C., 2011. Remote sensing land surface temperature for meteorology and climatology: a review. *Meteorol. Appl.* 18, 296–306. <https://doi.org/10.1002/met.287>.
- Varentsov, M., Konstantinov, P., Baklanov, A., Esau, I., Miles, V., Davy, R., 2018. Anthropogenic and natural drivers of a strong winter urban heat island in a typical Arctic city. *Atmos. Chem. Phys.* 18, 17,573–17,587. <https://doi.org/10.5194/acp-18-17573-2018>.
- Yakovlev, B., 1972. A.: *The Climate of Murmansk*, Gidrometeoizdat. Leningrad, 108 pp.
- Yang, Y., Cai, W., Yang, J., 2017. Evaluation of MODIS land surface temperature data to estimate near-surface air temperature in Northeast China. *Remote Sens.* 9, 410. <https://doi.org/10.3390/rs9050410>.
- Zhang, X., Friedl, M.A., Schaaf, C.B., Strahler, A.H., Schneider, A., 2004. The footprint of urban climates on vegetation phenology. *Geophys. Res. Lett.* 31 (12) <https://doi.org/10.1029/2004GL020137>.
- Zhao, L., Lee, X., Smith, R.B., Oleson, K., 2014. Strong contributions of local background climate to urban heat islands. *Nature* 511, 214–219. <https://doi.org/10.1038/nature13462>.

Victoria Miles is a researcher at the Nansen Environmental and Remote Sensing Center (NERSC) Bergen, Norway with a specialization in boreal ecology and remote sensing. Her current research efforts are in the arctic and boreal ecosystems. She is examining the recent dynamic of urban climate with connection to natural environmental and climatic factors.

Igor Esau is a professor at Institute of Physics and Technology, UiT, The Arctic University of Norway, Tromsø, Norway. His primary scientific interest is to investigate links between small scale and global scale processes. Specifically, he focuses on understanding on the role played by the stably stratified boundary layers in regulating the air quality, micro-climate and connections between the large-scale circulation and micro-physics of the Earth's climate system.

Martin Miles is a researcher at NORCE Norwegian Research Centre, Bergen, Norway, and the Institute of Arctic and Alpine Research (INSTAAR), University of Colorado, Boulder, USA. His primary research interest is to investigate climate variability on interannual to centennial time scales. Specifically, he focuses on the role of arctic sea ice and ocean variability on regional climate-system variability and climate transitions.